Spatiotemporal averaging of in-stream solute removal dynamics

Nandita B. Basu,[1] P. Suresh C. Rao,[2] Sally E. Thompson,[3] Natalia V. Loukinova,[1] Simon D. Donner,[4] Sheng Ye,[5] and Murugesu Sivapalan[5,6]

Received 1 November 2010; revised 24 March 2011; accepted 18 April 2011; published 15 July 2011.

[1] The scale dependence of nutrient loads exported from a catchment is a function of complex interactions between hydrologic and biogeochemical processes that modulate the input signals from the hillslope by aggregation and attenuation in a converging river network. Observational data support an empirical inverse relation between the biogeochemical cycling rate constant for nitrate k (T^{-1}) and the stream stage h (L), $k = v_f/h$, with v_f, the uptake velocity (LT^{-1}), being constant in space under steady flow conditions. Here we offer a physical explanation for the persistence of this pattern across scales and then extend the analysis to spatiotemporal scaling of k under transient-flow conditions. Inverse k-h dependence arose as an emergent pattern by coupling the mechanistic Transient Storage Model with a network model. Analytical modeling indicated that (1) nitrate processing efficiency increases with increasing variability in the discharge Q and (2) temporal averaging had no effect on the exponent a of the k-h relationship ($k = v_f/h^a$) in catchments with low Q variability, but strong dependence arose in catchments with high variability in Q. Network modeling in domains with low Q variability confirmed that the exponent a was independent of temporal averaging, but v_f was a function of the averaging timescale. The probability distribution functions for k could be adequately predicted using analytical approaches. Understanding the k-h scaling relationships enables the direct estimation of the variability in nutrient losses due to in-stream reactions without requiring explicit information for spatially distributed network modeling.

Citation: Basu, N. B., P. S. C. Rao, S. E. Thompson, N. V. Loukinova, S. D. Donner, S. Ye, and M. Sivapalan (2011), Spatiotemporal averaging of in-stream solute removal dynamics, *Water Resour. Res.*, *47*, W00J06, doi:10.1029/2010WR010196.

1. Introduction

1.1. Background and Motivation

[2] Human impacts on the landscape are manifested in streams and receiving water bodies that integrate inputs of water and solutes from spatially extensive drainage areas [*Galloway et al.*, 2008; *Gruber and Galloway*, 2008]. Water-quality deterioration and impairment of aquatic ecosystem habitats follow human impact gradients reflected in increased agricultural, urban, and industrial activities. Ecosystem impacts include chronic effects driven by accumulated nutrient loads (e.g., coastal hypoxia), acute effects generated by exposure of aquatic biota to high pollutant concentrations, and hydrologic alterations to the lotic habitat. Increased nutrient loads delivered from watersheds due to agricultural intensification, industrialization, and urbanization have contributed to the persistence of large hypoxic zones in inland and coastal waters at a global scale [e.g., *Smith*, 2003; *Diaz and Rosenberg*, 2008; *Kemp et al.*, 2009; *Rabalais et al.*, 2009; *Osterman et al.*, 2009; *Rabalais et al.*, 2010]. Agricultural activities have also contributed to pesticide pollution that is associated with birth defects and reproductive problems [*Winchester et al.*, 2009; *Fuortes et al.*, 1997]. Of more recent concern are the emerging contaminants (pharmaceuticals; synthetic and natural hormones) that are generated from land application of animal manures near Concentrated Animal Feeding Operations (CAFOs), and by discharges from municipal wastewater treatment plants [*Soto et al.*, 2004; *Durhan et al.*, 2006].

[3] Numerous factors must be accounted for in order to predict the environmental fate and transport of these solutes: (1) the "source function" which characterizes the spatial distribution and magnitudes of the sources; (2) the release dynamics, i.e., mobilization as determined by the interaction between biogeochemical and hydrologic processes; and (3) the "reactivity" of the constituents (sorption, transformations, uptake, etc.) while being transported through the vadose zone, saturated zone (groundwater) and the stream network.

[4] This paper focuses on the modification of solute loads exported along stream networks, as a result of (1) aggregation of loads from contributing subwatersheds and (2) attenuation resulting from biogeochemical uptake or transformation in the stream. Persistence and transport of chemicals in stream networks is controlled by complex interactions between the biogeochemical attenuation processes (e.g., sorption, abiotic and biotic transformations) occurring in the water column and

[1]Department of Civil and Environmental Engineering, University of Iowa, Iowa City, Iowa, USA.
[2]School of Civil Engineering and Department of Agronomy, Purdue University, West Lafayette, Indiana, USA.
[3]Nicholas School of the Environment, Duke University, Durham, North Carolina, USA.
[4]Department of Geography, University of British Columbia, Vancouver, British Columbia, Canada.
[5]Department of Geography, University of Illinois at Urbana-Champaign, Urbana, Illinois, USA.
[6]Department of Civil and Environmental Engineering, University of Illinois at Urbana-Champaign, Urbana, Illinois, USA.

0043-1397/11/2010WR010196

sediments, and the hydrologic transport processes (e.g., water flow, hyporheic exchange) that propagate solute loads [*Boyer et al.*, 2006]. A substantial body of literature on in-stream processing at multiple spatiotemporal scales is available for nitrogen, and thus our framework and analyses are focused on nitrate.

1.2. Metrics for In-Stream Nitrate Loss

[5] Nitrate loss in streams is commonly described by an "in-stream removal" metric, defined as a function (R) of the load exported by the stream (Φ_{out}), and the load delivered from the landscape to the stream (Φ_{in}):

$$R = 1 - \frac{\Phi_{out}}{\Phi_{in}} \quad (1)$$

R ($0 < R < 1$) varies with the specific temporal (e.g., daily, monthly, seasonal or annual) and spatial (e.g., reach or catchment) scales of averaging. Normalization by input loads in equation (1) accounts for variations in land use, so that R primarily represents the scaling of nitrate loads arising from in-stream processes.

[6] Although a number of physical-chemical processes drive nitrate losses in streams, the cumulative effects of these processes are traditionally described using first-order kinetics [*Alexander et al.*, 2000; *Boyer et al.*, 2006]. At the scale of a single reach, and assuming first-order removal kinetics, R can be described as a function of the first-order biogeochemical cycling rate constant k (T^{-1}) and the mean hydraulic residence time within the reach τ [T] (= L/u; where L is the length of the reach, and u [L/T] is the stream velocity):

$$R = 1 - \exp(-k\tau) \quad (2)$$

The two dominant processes that remove nitrate from streams are biotic uptake in the water column, and denitrification within the anoxic sediment [e.g., *Doyle*, 2005; *Böhlke et al.*, 2008]. Of these, denitrification is the primary process contributing to the net removal of N within the river network [*Wollheim et al.*, 2006; *Boyer et al.*, 2006]. Assimilatory processes (e.g., plant uptake) result in temporary removal of nitrate, but mineralization eventually releases the nitrogen back to the water column [*Wollheim et al.*, 2006].

[7] For this study we focus on denitrification, and in the rest of the manuscript k will be used to denote the effective rate constant for denitrification. The parameter k represents the combined effect of mass transfer rates across the sediment-water interface and denitrification rates in the stream sediment. Significant spatial variability has been documented in these rates as a function of stream sediment characteristics, local gradients, availability of carbon, and redox conditions [*Inwood et al.*, 2005; *Arango et al.*, 2007; *Arango and Tank*, 2008; *Mulholland et al.*, 2008; *Battin et al.*, 2008]. Despite this complexity, several experimental studies conducted under steady flow (base flow) conditions have shown that the first-order denitrification rate constant varies inversely with stream stage h [L]; $k = v_f/h$, with v_f, the uptake velocity (LT^{-1}) being essentially constant [*Alexander et al.*, 2000; *Doyle et al.*, 2003; *Wollheim et al.*, 2006; *Ensign and Doyle*, 2006; *Alexander et al.*, 2009; *Marcé and Armengol*, 2009].

[8] A constant v_f has been attributed to decrease in the volume of the anoxic sediment zone relative to the water column with increase in stream depth [*Wollheim et al.*, 2006; *Botter et al.*, 2010]. However, a quantitative explanation of the observed stage dependence of k, and an analysis of the expected variability of v_f as a function of the mass transfer and the denitrification parameters is largely lacking. The inverse stage dependence of k has interesting implications for scaling of solute loads. Stream discharge and stage vary in space (along a stream network), as well as in time (transient flow in response to storm events) at any reach within the network, leading to spatiotemporal fluctuations in k. While the scaling behavior of hydrologic variables (e.g., Q, h, τ) along a stream network has been studied extensively [*McKerchar et al.*, 1998; *Rodriguez-Iturbe and Rinaldo*, 1997], the scaling relationships of biogeochemical processing (manifested in k) have not been well explored [*Alexander et al.*, 2000].

1.3. Objectives and Organization

[9] This paper explores the scale dependence of the biogeochemical cycling rate constant (k; T^{-1}) along a stream network, and the relative role of hydrologic and biogeochemical controls on k. Three key questions drive the analysis.

[10] 1. What are the underlying process level explanations for the persistence of the observed inverse relationship between k and h for nitrate attenuation dynamics in streams?

[11] 2. How do reach-scale k-h relationships, measured under *steady-flow* conditions, vary with spatial and temporal averaging through aggregation along a converging stream network during *transient-flow* conditions?

[12] 3. Can the intra-annual variability in hydroclimatic forcing coupled with hydrologic and biogeochemical controls be used to predict the intra-annual variation in k?

[13] Answering question 1 (section 4) would help to bridge the gap between mechanistic approaches used at the reach scale and empirical approaches used at the network scale (see section 2.2 for further details). It would also provide insight into the expected range of v_f values based on measurable stream attributes (e.g., mass transfer rate across the sediment water interface, and denitrification rate constant in the sediment). Question 2 (section 5) has important implications for the prediction of in-stream solute losses due to biogeochemical processes. We hypothesize that if indeed scale-dependent relationships emerge, predicting such losses may be possible using analytical approaches, avoiding the need to use spatially distributed stream network models. Finally, answering Question 3 (section 6) would enable the estimation of the probability density functions (pdf's) to characterize the mean and variability in nutrient removal, based only on estimates of known climatic and anthropogenic forcing. Before we address these three questions explicitly, a conceptual framework to permit analysis of the problem is developed in section 2 and the methodology is described in section 3.

2. Conceptual Framework

2.1. Hydrologic Versus Biogeochemical Controls on Nitrate Removal Dynamics

[14] Denitrification occurs primarily in the anoxic stream sediment, which is supplied with nitrate from the water column by mass transfer across the sediment-water interface [*Stream Solute Workshop*, 1990]. These interactions can be quantified using the transient storage model (TSM), first

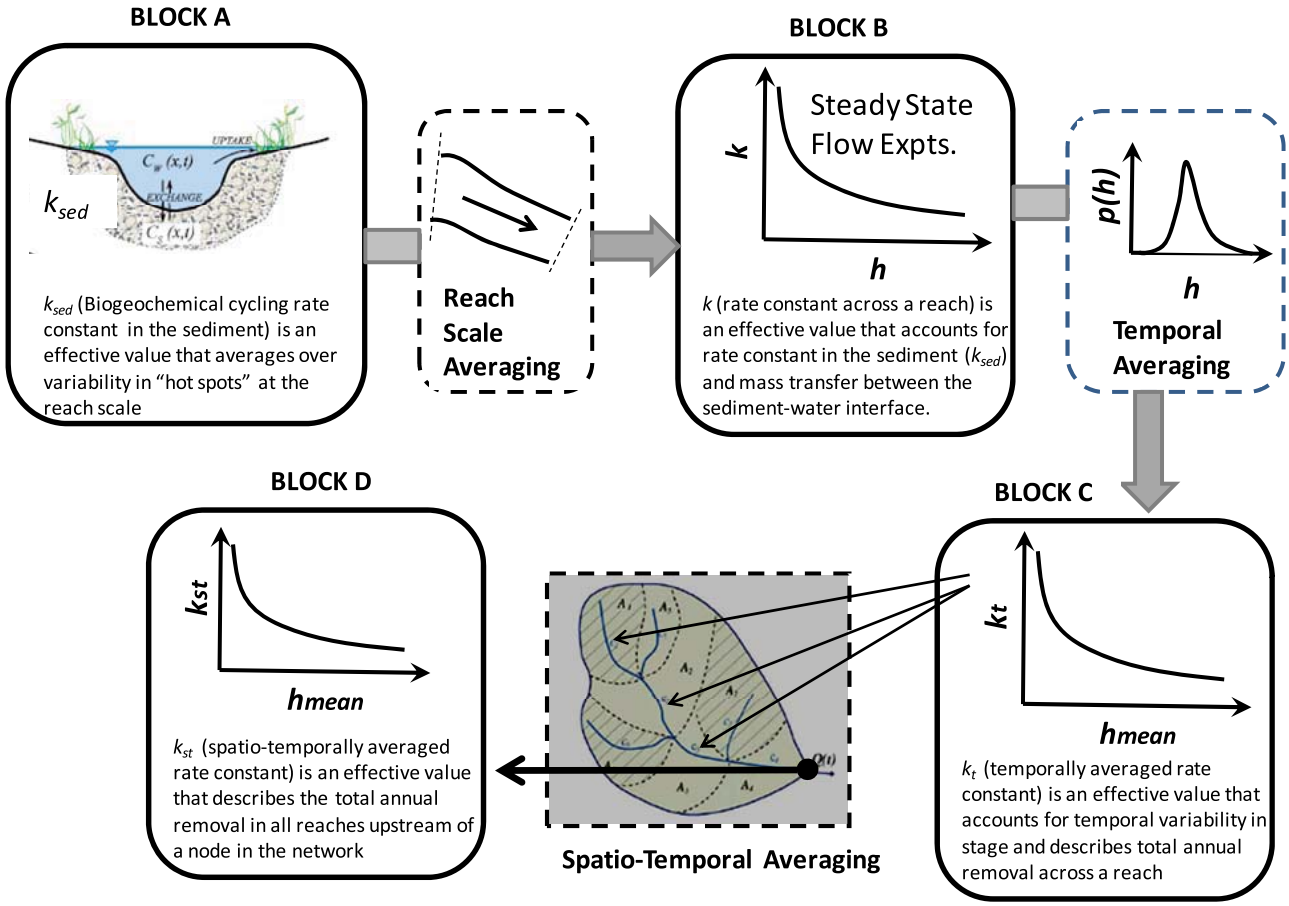

Figure 1. Schematic showing spatiotemporal averaging of reaction rate constants along the stream network.

proposed by *Bencala and Walters* [1983], and extensively used since then in tracer studies in streams [*Wagner and Gorelick*, 1986; *Hart*, 1995; *Green et al.*, 1994; *Runkel and Chapra*, 1993; *Harvey et al.*, 1996; *Marion et al.*, 2003, 2008]. Block A in Figure 1 is a schematic representation of the two-compartment TSM model that describes reach-scale concentration dynamics as a function of the mass transfer rate constant α [T^{-1}] at the sediment-water interface, and the denitrification rate constant in the stream sediment k_{sed} [T^{-1}]. Note that k_{sed} and α can vary spatially within a reach, and the values used here are average values for over reach.

[15] The TSM approach described above has been extensively used at the reach scale to interpret reactive and nonreactive tracer data [*Mulholland and DeAngelis*, 2000; *Thomas et al.*, 2003; *Tank et al.*, 2008]. At catchment scales, however, nitrate transport modeling is primarily based on empirical relationships ($k = v_f/h$). The lack of a mechanistic link between the two scales makes applying reach-scale experimental data to catchment-scale predictions challenging. *Botter et al.* [2010] attempted to establish a link between reach and catchment scales by deriving a functional form for the k-h relationship from TSM. However, their analysis was limited by assumptions of steady state, and specific functional form for the mass transfer rate.

[16] Here, we will expand on their work by solving the coupled reach-scale TSM equations under steady and transient flow conditions, to estimate R and k (using equation (1)) by making reasonable assumptions regarding the mean travel time (see section 3). The k (block B in Figure 1) thus estimated represents the combined effects of the mechanistic hydrologic (α) and biogeochemical (k_{sed}) parameters. Evaluating the expected range of the empirically defined k or uptake velocity ($v_f = kh$) for measured ranges of the mass transfer and denitrification parameters enables linking mechanistic and empirical approaches of solute removal dynamics.

2.2. Spatiotemporal Scaling of In-Stream Removal Along a River Network

[17] Because k depends on h, spatiotemporal fluctuations in flow conditions (Q or h) are propagated into k. Given that these Q and h fluctuations scale predictably through space and time [*Rodriguez-Iturbe and Rinaldo*, 1997], k should also display predictable scaling behavior. Establishing such relationships enable prediction of total annual in-stream removal at the reach and network scales, without using explicit distributed network models.

[18] A schematic of the spatiotemporal averaging scheme is presented in Figure 1 (blocks C and D). We start with a relationship between k and h measured under base flow scenarios (block B in Figure 1), then scale up in time (block C in Figure 1) to obtain a relationship between k_t (temporally averaged reaction rate constant) and h_{mean} (h_{mean} = mean annual (or, monthly) stage at any reach estimated from the mean annual (or, monthly) discharge and the stage-discharge

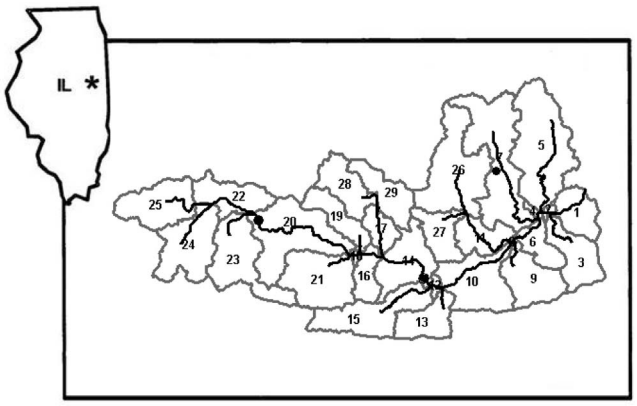

Figure 2. Map of the Little Vermilion River Basin in east central Illinois with 29 REWs delineated.

relationship), and scale up in space (block D in Figure 1) over a stream network to obtain a relationship between k_{st} (spatiotemporally averaged reaction rate constant) and h_{mean}. Note that for network-scale analysis, h_{mean} is the mean annual stage at the reach immediately upstream of the node at which the averages are estimated (i.e., a local value rather than a catchment-scale average value). The significance of these mean values for describing spatiotemporally averaged parameters will be discussed below.

[19] The temporally and spatiotemporally averaged reaction rate constants k_t [T^{-1}] and k_{st} [T^{-1}], respectively, are defined as

$$k_t = \frac{Ln(1 - R_t)}{\tau_t} \tag{3}$$

$$k_{st} = \frac{Ln(1 - R_{st})}{\tau_{st}} \tag{4}$$

where R_t and R_{st} are the fractional nutrient removal, as defined in equation (2), with the subscript t denoting the specified averaging timescale (here we use annual or monthly) for a given stream reach, and subscript st denoting averaging over all reaches upstream of a node in the network. In addition, τ_t and τ_{st} are the temporally and spatiotemporally averaged residence times, respectively. Scaling of k to estimate k_t and k_{st} requires an understanding of how to scale nutrient removal (R) and the residence time τ; this is accomplished using the results of a network model (section 5).

2.3. Probability Distribution Functions for k

[20] The intra-annual variability in k (as described by its pdf, $p(k)$) has received considerably less attention than descriptions of mean behavior [*Doyle*, 2005; *Marcé and Armengol*, 2009; *Hoellein et al.*, 2007; *Böhlke et al.*, 2008; *Botter et al.*, 2010]. Intra-annual variability of stream hydrologic conditions (e.g., frequency, duration and magnitude of the stream discharge) are directly controlled by the stochastic nature of the hydroclimatic forcing (rainfall patterns, potential evapotranspiration demands), and the spatial distribution of landscape attributes (soils, topography, vegetation) [*Botter et al.*, 2007a, 2007b, 2008, 2010]. The stochasticity in Q means that the stream depth (h) and the removal rate constant (k) are also random variables [*Botter et al.*, 2007a, 2007b, 2008, 2010]. *Botter et al.* [2010] examined the stochastic properties of the intra-annual variations in k in a stream reach, by linking rainfall forcing, landscape features, and stream geomorphology to in-stream processes. Assuming the streamflow pdf, $p(Q)$, to be a Gamma function, a power law relationship between stage and discharge ($h = mQ^n$; m and n are constants), and an inverse stage dependence of k, *Botter et al.* [2010] developed the following analytical expressions for the pdf of the stream stage, $p(h)$ and nutrient removal rate constant $p(k)$:

$$p(Q) = \frac{\gamma_Q^{\lambda/k_c} Q^{\lambda/k_c - 1} \exp(-\gamma_Q Q)}{\Gamma(\lambda/k_c)} \tag{5}$$

$$p(k) = \frac{\Omega(\Omega k)^{\left(-\frac{\lambda}{nk_c}-1\right)} \exp\left(-(\Omega k)^{-1/n}\right)}{\Gamma(\lambda/k_c) n} \tag{6}$$

where λ [T^{-1}] = frequency of streamflow producing rainfall events; k_c [T^{-1}] = inverse of mean catchment residence time; γ_Q [T/L^3] is the mean runoff; and $\Gamma(\lambda/k_c)$ is the complete Gamma function of the argument λ/k_c; $\Omega = 1/(\theta v_f)$; $\theta = \gamma_Q^n/m$ represents the inverse of the stage observed when the discharge is equal to the mean streamflow jump produced by the runoff events. The analytical equations developed by *Botter et al.* [2010] will be evaluated using results from the network model (section 6).

3. Methods

[21] Methods of analysis specific to the three key questions (see section 1.3) are presented below; overlap of methods between these questions was necessary to maintain clarity.

3.1. Mechanistic Basis for the Empirical k-h Relationship (Question 1)

[22] We used a dynamic network flow model, coupled with a two compartment (sediment and water) biogeochemical process model. The dynamic network flow model is based on the representative elementary watershed (REW) theory of *Reggiani et al.* [1998, 1999, 2001], while the biogeochemical process model is based on the upscaling of the TSM model equations for dissolved nutrients [*Bencala and Walters*, 1983; *Runkel*, 1998], with explicit inclusion of the interactions between the main water column and the sediment zone (S. T. P. Ye et al., Dissolved nutrient removal dynamics in river networks: A modeling investigation of transient flows and scale effects, submitted to *Water Resources Research*, 2011). The TSM equations are solved at the reach scale where the advection term and the lateral mass inflow term are replaced by solute mass input from upstream nodes, and mass output to downstream nodes. We thus neglect longitudinal variations within a reach, but consider this approximation to be reasonable since our interest lies at the network scale. The coupled model is implemented using a river network extracted from the digital elevation model available for Little Vermilion River Watershed, (LVRW) a 489 km^2 basin (Figure 2) in east central Illinois [*Mitchell et al.*, 2000; *Algoazany*, 2006]. Further details of the model and the site are presented by Ye et al. (submitted manuscript, 2011).

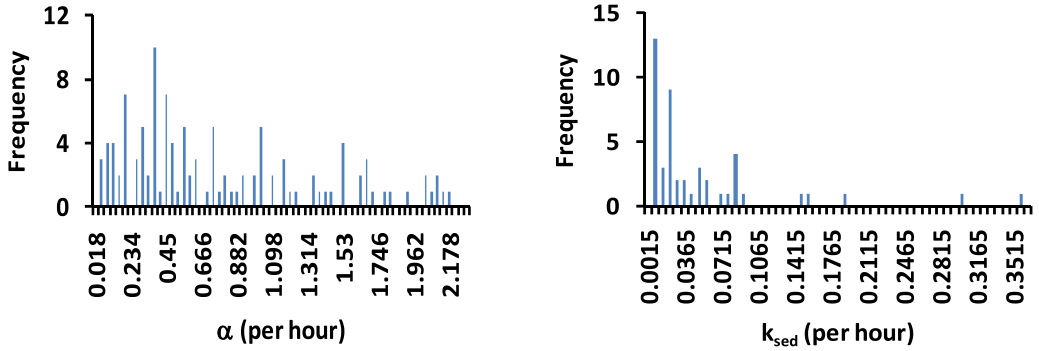

Figure 3. Distribution of experimental values for (left) the mass transfer exchange rate α and (right) the rate of denitrification in stream sediments (k_{sed}) [*Battin et al.*, 2008; *Mulholland et al.*, 2008].

[23] Model outputs were used to analyze the effects of the mass transfer rate constant α (T^{-1}), and the removal rate constant in the stream sediment k_{sed} (T^{-1}) on the resultant k-h relationship. We first explored this question under steady base flow (1 mm/d) conditions. The steady-flow simulations were expected to mimic the steady state stream tracer experiments that are the source of most of the available data, and simplify the system dynamics by omitting flood wave propagation. A constant input nitrate concentration of 5 mg/L was used to simulate typical ranges of nitrate concentration at base flow in the watersheds dominated by corn-soybean rotations in the Midwestern United States. [*Schilling and Libra*, 2000]. Note that given the assumption of linear reaction kinetics for denitrification, the choice of nitrate concentration has no effect on the first-order rate constant. The reach-scale removal R was estimated as the ratio of the solute mass lost in the reach and the mass delivered to that reach. The residence time (τ) was calculated using the reach length and Manning's equation for velocity. The rate constant k was estimated using equation (2), and expressed as $k = v_f/h^a$. Instead of implicitly assuming an empirical form of $v_f (= kh)$ [*Wollheim et al.*, 2006], we analyzed the simulation outputs to determine the v_f and a values that were the best fit to the model outputs. The variability in v_f and a was evaluated as a function of variations in α and k_{sed} for which a reasonable range of empirical values were obtained from the literature, as discussed below.

[24] *Battin et al.* [2008] provide a compilation of α (T^{-1}) values estimated in reach-scale tracer experiments in temperate, tropical, semiarid and Arctic streams (Figure 3, left). Across these diverse sites, α values follow an asymmetric distribution (range: 0.02–16 h^{-1}) with a modal value of 0.36 h^{-1}, and 80% of the values between 0.02 and 2 h^{-1}. Estimates of the reach-scale mean rate constant in the sediment k_{sed} (T^{-1}) are sparse in comparison to α. Most stream nutrient studies are focused on estimating the effective loss rate between two sampling locations, which provides an estimate of k, not k_{sed}. Our estimates of the behavior of k_{sed} are therefore based on a single large-scale nitrogen stable isotope study, the Lotic Intersite Nitrogen Experiment (LINX). LINX examined 72 representative reaches in North America to investigate in-stream N retention processes under base flow conditions [*Mulholland et al.*, 2008]. The estimated k values followed a strongly asymmetric distribution (Figure 3, right), with a range between 0.002 to 4.8 h^{-1}, and a mode of 0.01 h^{-1}; 80% of the values were between 0.002 and 0.08 h^{-1}. For our analysis, we used $\alpha = 0.025, 0.25, 1$ and 2.5 h^{-1} and $k_{sed} = 0.025, 0.1, 0.5$ and 2.5 h^{-1} to cover the range of values reported in the literature.

3.2. The k-h Scale Dependence (Question 2)

[25] We explored this question using models of varying levels of complexity: (1) analytical approach at the reach scale for the k_t-h_{mean} relationship, (2) mechanistic approach including Transient Network Simulations (TSM+REW) for k_t-h_{mean} and k_{st}-h_{mean} relationship, and (3) network modeling of the Mississippi-Atchafalaya River Basin (MARB) for the k_{st}-h_{mean} relationship. The three modeling approaches had different assumptions as discussed below. The convergence between these varying approaches suggests that the results are robust against variations in model assumptions and limitations. Experimental data to explore scale dependence of in-stream solute losses are largely lacking at the network scale, which forces this strong dependence on modeling analyses to draw inference at these scales.

[26] The analytical approach is based on using the pdf of Q (as defined by stochastic hydroclimatic controls) and the dependence of k and τ on Q to estimate the temporally averaged rate constant k_t at the reach scale. To do so we use equation (3) and the following definitions of R_t and τ_t:

$$R_t = \int p(Q)R(Q)dQ = \int p(Q)(1-\exp(-k\tau))dQ$$
$$= \int p(Q)\left(1-\exp\left(-\frac{v_f}{h}\frac{L}{u}\right)\right)dQ \quad (7)$$

$$\tau_t = \int p(Q)\tau(Q)dQ = \int p(Q)\left(\frac{L}{u}\right)dQ \quad (8)$$

[27] Here, power function relationships between h and Q ($h = mQ^n$; m and n are constants) and u and Q ($u = rQ^s$; r and s are constants) are used to describe the dependence of R and τ on the stream hydraulic variables. We assumed a Gamma distribution to describe $p(Q)$ (equation (5)) and calculated the mean stage h_{mean} using the mean discharge Q_{mean} and the stage-discharge relationship. The tractability of the analytical approach enabled an explicit comparison of the k_t-h_{mean} relationship across different catchment-climate regimes (as embodied in λ/k_c), as well as biogeochemical regimes (as embodied in v_f). Five values of $\lambda/k_c = 0.5, 1, 1.5, 2$ and 2.5 were used, representing a progression of decreasing variability in the streamflow distribution. Increases in

Table 1. Parameters of the Probability Distribution Function of k (Figure 11) for Watersheds in the Mississippi Basin [*Donner et al.*, 2004]

		Predicted		Fitted	
Watershed Name	Area (km^2)	λ/k_c	$1/\gamma_Q$ (m^3/s)	λ/k_c	$1/\gamma_Q$ (m^3/s)
Allegheny	29,098	2.8	183	0.6	2,415
Muskinghum	16,000	1.9	97	4.0	63
Rock	23,766	2.6	101	0.7	1,085
Iowa	32,224	2.2	150	0.8	6,89
Illinois	71,606	2.9	276	0.8	1,790
Tennessee	143,373	1.6	1,528	1.1	2,931
Yellowstone	179,341	2.7	96	1.5	137
Grand	19,878	2.0	88	0.8	441
Canadian	75,669	2.6	41	1.0	67

λ/k_c correspond to a decrease in the variability of $p(Q)$ (equation (5)), since the coefficient of variation of the Q distribution is given by $\sqrt{k_c/\lambda}$. Two uptake velocities $v_f = 10$ and 100 m/yr were used, based on a range of values drawn from data synthesis [*Wollheim et al.*, 2006]. Note that these rates represent removal by denitrification only, and are smaller than reported uptake velocities when both denitrification and biotic uptake within the water column are considered [*Doyle*, 2005]. Finally, we used m and n values of 0.3 and 0.4, and r and s values of 0.3 and 0.2 based on the average (over all reaches) scaling behavior predicted by the hydraulic model (REW) mentioned in section 3.1 and described in Ye et al. (submitted manuscript, 2011).

[28] The analytical approach is easily tractable, but required several simplifying assumptions that were relaxed in the two network numerical modeling approaches (approaches b and c; see above). The two network approaches were distinctly different in their model assumptions, as well as the scale of analysis. The mechanistic approach (approach b), as described in section 3.1, used the two-compartment TSM approach coupled to a dynamic flow model to describe the denitrification kinetics. The k_t-h_{mean} and k_{st}-h_{mean} relationships were estimated as functions of nested scales (2 km^2 – 489 km^2) in a single watershed, and for a single climatic regime representative of the humid Midwest United States. The empirical modeling (approach c), was done as a part of a separate study, and used the coupled IBIS-THMB Model [*Donner et al.*, 2002, 2004]. IBIS-THMB employs standard empirical approaches ($k = v_f/h$) to describe denitrification kinetics. The k_{st}-h_{mean} relationship was estimated at the outlet of large watersheds (>10,000 km^2; see Table 1 for details on individual watersheds), across different climatic regimes in the MARB system. The scale of resolution (~ 100 km^2) was much coarser in the MARB study making nested analysis similar to LVRW difficult. Variable discharge and concentration time series data from subwatersheds were used as inputs to the stream network model in both approaches. In LVRW, the model was run for 7 years, while in MARB the duration of the model run was 30 years.

[29] The reach- and network-scale effective rate constants (k_t and k_{st}) were calculated using equations (3) and (4), model outputs of R_t and R_{st}, and estimates of τ_t and τ_{st}. The temporally averaged residence time was calculated in approach b based on Manning's equation for velocity and the length of the reach. The spatiotemporally averaged residence time τ_{st} in approach b was estimated by considering the distribution of travel paths to a node, and the mean travel times along those paths (Ye et al., submitted manuscript, 2011). The spatiotemporally averaged residence time τ_{st} in approach c was based on simple scaling relationships that exist between residence times and upstream contributing area ($\tau = -0.0065 + 0.2642A^{1/3}$, τ is the residence time in days and A is the upstream contributing area in km^2 [*Alexander et al.*, 2000]).

3.3. The Probability Distribution Function of k (Question 3)

[30] *Botter et al.* [2010] developed an analytical expression to describe the intra-annual probability distribution function of k as a function of underlying climatic, hydrologic and biogeochemical controls (see equation (5)). The outputs from the MARB analysis were used to explore the predictive capacity of this analytical approach (section 6). The distribution of k_{st} values estimated using R_{st} and τ_{st} in the MARB analysis were used to plot the intra-annual pdf of k. To evaluate the predictive capacity of the analytical approach, we fitted the monthly discharge data to gamma distributions, and estimated γ_Q and λ/k_c (Table 1). The estimated γ_Q and λ/k_c, and the mean exponent and coefficient of the monthly k_{st}-h_{mean} relationship were then used to predict the pdf of k.

4. Mechanistic Basis for the Empirical *k-h* Relationship

[31] Process level controls on the experimentally observed k-h relationship were investigated by coupling a reach-scale mechanistic model with a spatially explicit network model. The statistical distributions for α and k_{sed} derived from the literature were asymmetric (Figure 3), prompting us to select the mode value (α = 0.36 h^{-1}; k_{sed} = 0.01 h^{-1}) for model simulations. The reach-scale removal is presented as function of increasing discharge for first-, second- and third-order streams along the river network in LVRW (Figure 4). As expected, R decreases with increase in Q because the sediment-water contact area is proportionally smaller, resulting in smaller in-stream losses (Figure 4). Methods outlined in section 3.1 were used to estimate k from R (Figure 5). We found the k-Q relationship to be well described by a power function ($k = 1.97Q^{-0.44}$; $R^2 = 0.91$). Further, for this network, the imposed hydraulics dictated the existence of a power-function relationship between reach-scale h (m) and Q (m^3/s)

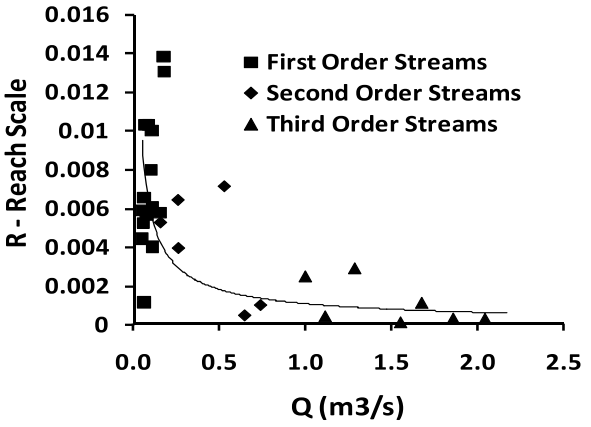

Figure 4. Relationship between reach scale R and Q for different stream orders. Simulation results are based on the network model in the Little Vermilion River Watershed.

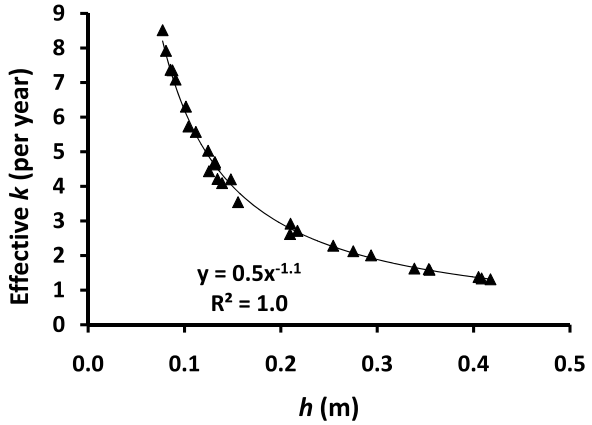

Figure 5. Emergent power function relationship between the effective k and stage h at the reach and catchment scale. Note that the observed inverse dependence arises in the reach scale relationship, while the network scale relationship has a smaller exponent. Simulation results are based on the network model in the Little Vermilion River Watershed.

($h = 0.29Q^{0.41}$; $R^2 = 0.94$), which resulted in an inverse dependence of k on h ($k \sim 0.5/h^{1.1}$). This result, with $a = 1.1$, is consistent with the empirical observations of an inverse dependence of reach-scale removal rate constant on the stream stage [*Alexander et al.*, 2000].

[32] The effect of the range of values of α and k_{sed} (Figure 3) on the resultant k-h relationship was explored (Figure 6). The exponent a value varied over a narrow range (0.9 to 1.1), despite 2 orders of magnitude variation in α and k_{sed} (Figure 6b). The uptake velocity v_f was nearly independent of α, but varied linearly with k_{sed} (Figure 6a). To explore the coupled effects of the two rate constants, we defined the nondimensional term k_{sed}/α to quantify the role of hydrologic (α) versus biogeochemical attributes (k_{sed}) in describing the resultant stage dependence. The exponent a was closer to 1 for very high (>10) and very low (<0.1) values of the ratio k_{sed}/α, and clustered around 1.1 for intermediate values (Figure 6c).

5. The *k*-*h* Scale Dependence

[33] Having established that the empirical k-h relationship emerges as a result of the controls on the mass transfer exchange between the stream and the transient storage zone, we now explore how this relationship scales up over a river network to generate effective relationships in time (k_t-h_{mean}; block C in Figure 1) and space (k_{st}-h_{mean}; block D in Figure 1).

5.1. Temporal Averaging at the Reach Scale (k_t)

5.1.1. Analytical Approach Based on Empirical k-h Function

[34] The temporally averaged rate constant k_t decreases with an increase in the mean stage (h_{mean}), and the rate of decrease is a function of hydrologic (λ/k_c) and biogeochemical (v_f) controls (Figure 7). For the same mean annual discharge, increase in the variability in Q (or, decrease in λ/k_c) leads to greater in-stream nutrient processing (larger k_t). Although the analytical expression for the k_t-h_{mean} relationship is complex, this relationship was reasonably approximated by a power law ($R^2 > 0.98$). For streams in which $\lambda/k_c > 1$ (hereafter referred to as "damped" systems owing to the lower intra-annual variability in Q), both the best fit coefficient ($v_{f,t}$) and exponent (a_t) of the power function fit to the k_t-h_{mean} relationship were approximately the same as those of the underlying k-h relationship (Table 2). In contrast, in streams with $\lambda/k_c < 1$ (hereafter referred to as "flashy" systems owing to the greater intra-annual variability in Q), a_t was smaller and $v_{f,t}$ was greater than the parameters of the k-h relationship. The rate of change of a_t and $v_{f,t}$ was highly

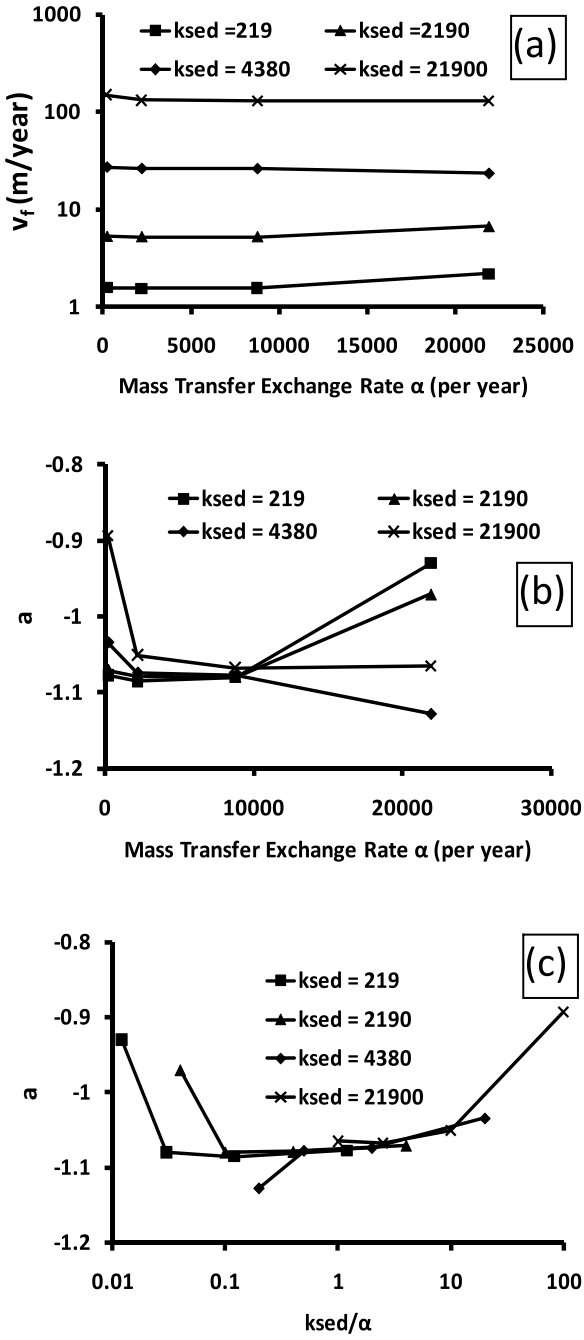

Figure 6. Variation of the coefficients and exponents of the $k = v_f/h^a$ relationship as a function of α and k_{sed} (a) v_f as a function of α; (b) a as a function of α; and (c) a as a function of k_{sed}/α. Simulation results are based on the network model in the Little Vermilion River Watershed.

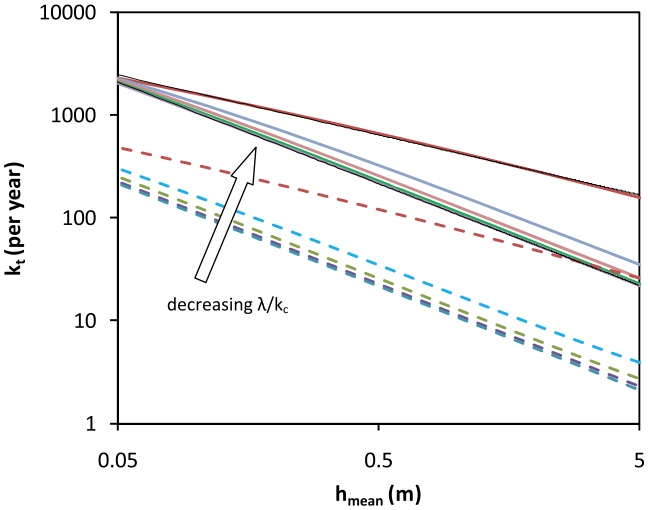

Figure 7. Analytical modeling used to derive the k_t-h_{mean} relationship for λ/k_c = 0.5, 1, 1.5, 2, and 2.5 and v_f = 10 m/yr (dashed lines) and 100 m/yr (solid lines). Power functions are fitted to the k_t-h_{mean} relationship, and the resulting exponents and coefficients are presented in Table 2. Results show that the k-h relationship does not change with temporal averaging in wet ($\lambda/k_c > 1$) domains but is significantly affected by averaging in dry domains ($\lambda/k_c < 1$).

nonlinear (Table 2) and greater for the smaller v_f (=10 m/yr). These results indicate the emergence of scale independence in "damped" streams, while strong nonlinearity and scale dependence might be more characteristic of "flashy" streams. This arises due to the strong asymmetry in $p(Q)$ in flashy streams that leads to h_{mean} not being the representative stage.

5.1.2. Mechanistic Approach (TSM+REW)

[35] The reach-scale k_t-h_{mean} relationship (Figure 8a) for different reaches along the stream network in LVRW was estimated using outputs from the mechanistic network model (TSM + REW) and the methods outlined in section 3.2. With increasing contributing area along the nodes of the network, h_{mean} increases, resulting in a decrease in k_t. We compare results obtained under steady-flow scenarios with transient-flow simulations using monthly and annual averaging. For both the monthly and annual averaging, all 7 years of data collapsed to yield a unique k_t-h_{mean} power-function relationship (Figure 8a). The exponent of the relationship was similar for both averaging time scales and equal to the exponent of the steady-flow relationship, suggesting emergence of temporal-scale invariance. The coefficient ($v_{f,t}$) was similar for the steady flow and the monthly averaging scenarios, but lower for the annual averaging scenario. This

Table 2. Exponents (a_t) and Coefficients ($v_{f,t}$) of the Power-Function Fit to the k_t-h_{mean} Relationship Function of Temporal Averaging Using the Analytical Approach

	a_t		$v_{f,t}$	
λ/k_c	v_f = 10	v_f = 100	v_f = 10	v_f = 100
0.5	0.63	0.59	46	274
1.0	0.95	0.90	18	183
1.5	0.98	0.98	9	91
2.0	1.00	1.00	9	91
2.5	1.00	1.00	9	91

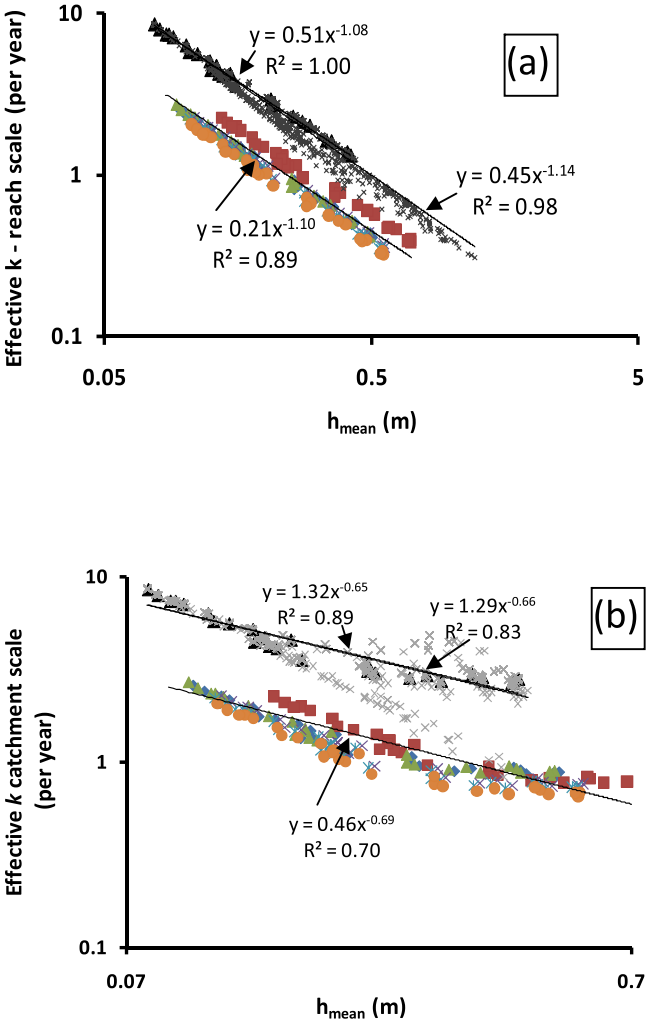

Figure 8. Relationship between the effective k and mean stage at (a) the reach scale and (b) the catchment scale. Simulation results are based on the network model in the Little Vermilion River Watershed. Black triangles represent the base flow scenario, black crosses represent monthly outputs from the transient simulations, and colored symbols represent annual outputs from the transient simulations. Each color indicates a different year, while each data point indicates a different reach for reach scale analysis and a different node in the network for catchment scale analysis.

difference is attributed to the carryover of residual nitrate in the stream sediments across averaging periods, as discussed below.

[36] Carryover refers to the fraction of the nitrate that is retained in the system (particularly in stream sediments) between averaging periods. It arises from the residence time of some of the nitrate being greater than the averaging time-scale. We found significant carryover of nitrate both in the steady and the transient flow simulations, especially at annual time scales. This led to the total nitrate removal being greater than the nitrate input into the stream network for some years. While carryover between adjacent time periods is plausible, observations of removals exceeding inputs are anomalous from a mass balance perspective. To correct for this effect, we initialized the model at the start of every year to run with zero nitrate in the sediment. We attribute the lower $v_{f,t}$ at the

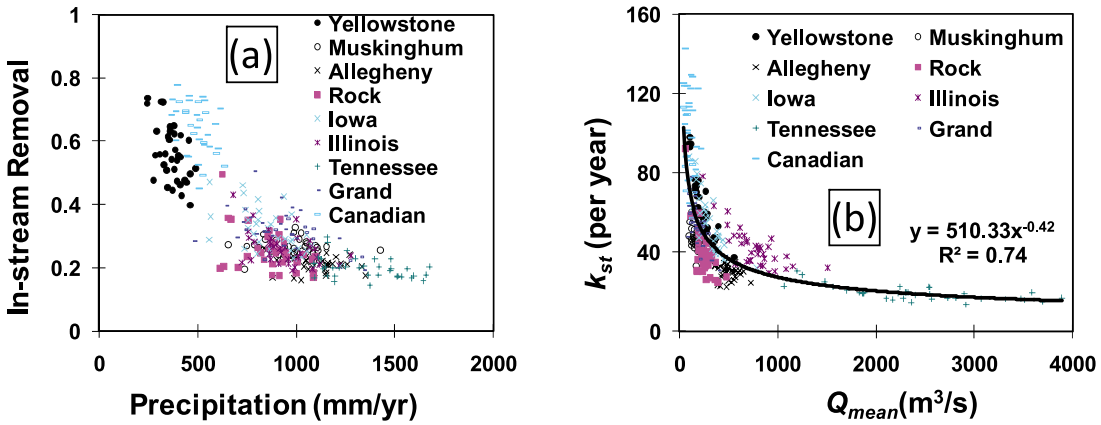

Figure 9. Mississippi Basin simulations by *Donner et al.* [2004]: (a) in-stream removal decreases with increase in precipitation and (b) collapse of all basins to yield a single relationship between effective k and Q.

annual time scale as being due to this initialization. A lower coefficient indicates that there was less removal at the annual time scale than at monthly scales, which occurs because we neglect the effect of potential removal of the carryover nitrate from the previous year. There is little data on carryover in the field because most reach-scale studies are short-duration experiments. Previous modeling studies did not encounter the carryover effect since they were based on empirical functions for nitrate removal in the stream sediment. Our results indicate that carryover does not affect the exponent of the *k*-*h* relationship, but does affect the magnitude of the uptake velocity. Sensitivity of the uptake velocity to the carryover fraction, and existence of carryover in field studies need to be explored in further detail in future work.

5.2. Spatiotemporal Averaging at the Network Scale

5.2.1. Mechanistic Approach (Based on TSM+REW)

[37] The network-scale k_{st}-h_{mean} relationship (Figure 8b) along the LVRW stream network is estimated using outputs from the mechanistic network model (TSM + REW) and the methods outlined in section 3.2. We compare results obtained under steady-flow scenario with transient-flow simulations using monthly and annual averaging (Figure 8b). The exponent of the k_{st}-h_{mean} relationship was similar between steady- and transient-flow simulations, but lower than the exponent of the k_t-h_{mean}. The smaller value of the exponent of the k_{st}-h_{mean} relationship compared to the k_t-h_{mean} relationship is attributed to the greater processing that occurs at the network scale because of the longer residence time. Similar to the observations for temporal averaging, $v_{f,t}$ values were similar for monthly averaging and steady-flow scenarios, but lower for annual averaging. We attribute this effect to carryover of residual nitrate, as discussed in section 5.1.2.

5.2.2. Empirical Approach (Based on *Donner et al.* [2004])

[38] *Donner et al.* [2004] presented the results from basin-scale simulations for percent annual in-stream removal of nitrate as a function of basin-averaged precipitation (*P*). They noted an inverse relationship between nitrogen removal and increasing precipitation (Figure 9a). Despite the presence of this general pattern of inverse dependence across watersheds in different climatic regimes, the specific *R*-*P* relationship appeared to be watershed specific, with similar precipitation leading to different removal fractions in different watersheds. In contrast to basin specific patterns of *R*-*P*, the k_{st}-Q_{mean} relationship for all nine watersheds collapsed to yield a single power function with an exponent of 0.42 (Figure 9b). This collapse of seemingly diverse watershed nitrate removal behaviors in large basins across a range of climatic types, to generate a single effective k_{st}-Q_{mean} relationship is striking, and indicates that it might be possible to estimate basin-scale in-stream nutrient losses without explicit spatial network analysis. It also implies that hydrologic filtering (the conversion of precipitation to streamflow by filtering through the landscape) governed the variability in nutrient removal across watersheds.

[39] The corresponding k_{st}-h_{mean} relationship, plotted using a stage discharge relationship $h = 0.26Q^{0.4}$ (based on a study of 112 river locations in the United States, *Leopold and Maddock* [1953]), yielded an approximate inverse stage dependence (Figure 10). Consistent with our previous observation (approach b), the exponent of the k_{st}-h_{mean} relationship was independent of the averaging timescale, but the coefficient varied with averaging (Figure 10). In contrast to the mechanistic approach (approach b) described before, the coefficient here is greater at the annual time scale than the monthly time scale. The mechanistic approach had the carryover effect that is absent in the empirical approach used by *Donner et al.* [2004]. Here, the differences in the coefficients at the two averaging time scales arise from the assumption of h_{mean} being the representative stage. The total annual removal at any node in a watershed is the sum of removal through all pathways (from all first-order subwatersheds) leading to that node. During travel through any of these pathways, channels of increasing depth and decreasing removal efficiency is encountered. It is intuitively obvious that the representative stage would be lower than the mean stage at the outlet, which is the largest stage encountered along any of the pathways from source to outlet. A representative stage at the watershed scale will be a function of the hydroclimatic controls, and the network topology and geomorphology that defines the distribution of stage throughout the network. However, the exact functional relationship between the mean stage at the outlet and the spatiotemporal distribution of stages requires further analyses and is beyond the scope of this work.

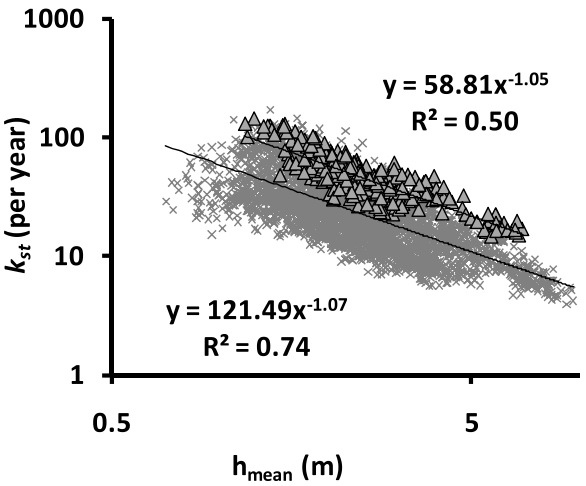

Figure 10. Relationship between the effective k_{st} and h_{mean} at annual (triangles) and monthly timescales (crosses). Results are based on Mississippi Basin simulations by *Donner et al.* [2004].

6. Probability Distribution Function of *k*

[40] Having explored basin-wide scaling of k using semi-empirical models and uncovering a remarkably convergent behavior at monthly and annual averaging timescales, we next explored if the intra-annual pdf of k could be predicted as a function of the underlying climate, hydrologic and geomorphic controls in the system. As proposed by *Botter et al.* [2010], the pdf of k can be described by a Gamma distribution using parameters of $p(Q)$ and the k-Q relationship (equations (5) and (6)). The discharge pdf's could be described well by gamma distributions with λ/k_c ranging between 2 and 2.4 (Table 1). These parameters were able to reasonably capture the intra-annual pdf of k using the stochastic model proposed by *Botter et al.* [2010] (Figure 11). Of the nine basins explored in this study, the *Botter et al.* [2010] approach predicted the pdf's for some basins better than others. However, no definite correlation could be established between the distribution of Q and the predictive ability of the stochastic model. In addition to prediction, we fitted the pdf of k which as expected describes the numerical results better (Figure 11).

7. Discussion

7.1. Persistence of the Inverse Stage Dependence of *k*

[41] We investigated process controls on the experimentally observed inverse stage dependence of the denitrification rate constant k. Our results showed that over 2 orders of magnitude variation in the mass transfer exchange rate (α) and the sediment denitrification rate constant (k_{sed}), the exponent, a, of h in the $k = v_f/h^a$ relationship varied only between 0.9 and 1.1, thus validating the empirical results that assume $a \sim 1$. The inverse relationship was robust and insensitive to wide range of variations in two key sediment characteristics: α and k_{sed}. The robustness of the relationship is attributed to the mass transfer constraints to hyporheic

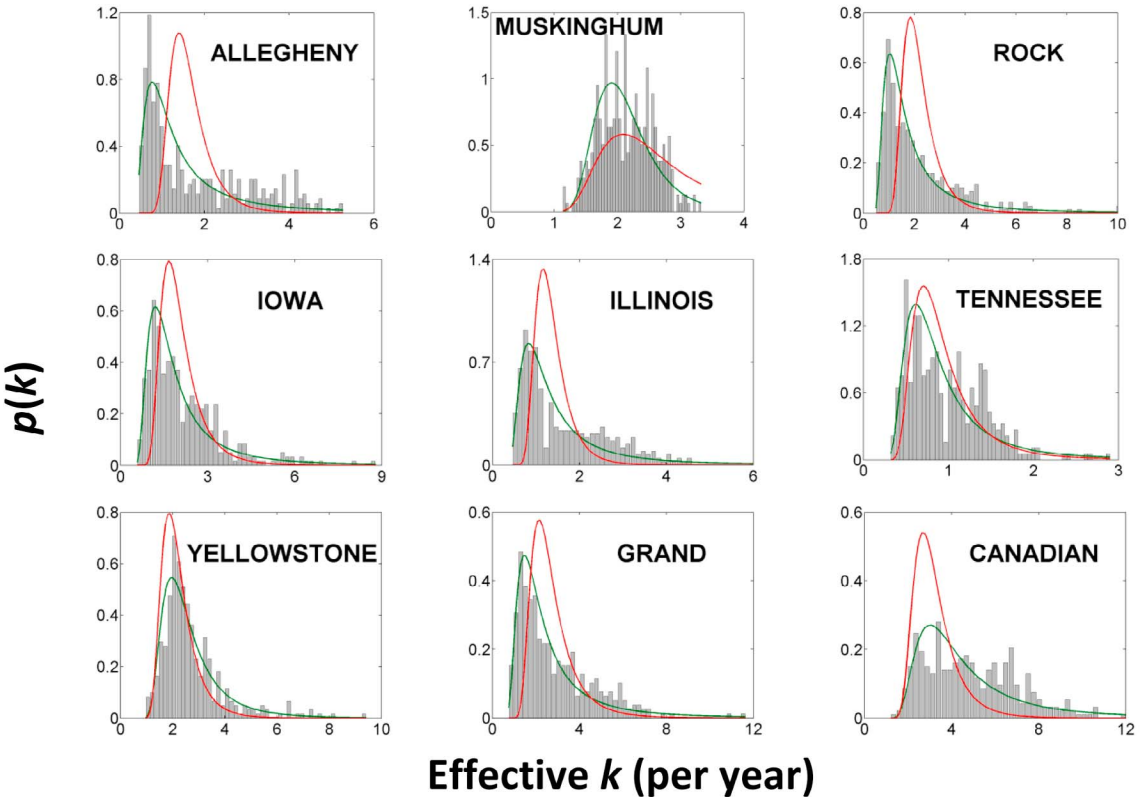

Figure 11. Probability distribution functions of the first-order effective rate constant for nine large basins in MARB. Histograms indicate simulation results from *Donner et al.* [2004], the red line is the predicted distribution from *Botter et al.* [2010], and the green line is the fitted distribution.

exchange being the rate-limiting step for removal, such that the system becomes comparatively insensitive to local biogeochemical attributes. The TSM approach explicitly accounts for the reduction in the proportion of the anoxic zone relative to the water column (which determines the mass transfer conditions) by simulating the flow dynamics in the channel cross section. The observation that varying α and k_{sed} had minimal effect on the k-h dependence quantitatively supports the hypothesis that he dynamics of change in contact volume (as manifested in stage) leads to the persistence of the inverse relationship.

[42] We further evaluated the sensitivity of the empirical uptake velocity v_f to the measured mass transfer and denitrification parameters. Estimated uptake velocities from our model results ranged between 2 and 200 m/yr, while observed v_f values across MARB have been observed to be fairly consistent at ~ 60 m/yr [*Wollheim et al.*, 2006]. Our modeling results indicated that v_f was insensitive to α, but increased linearly with increase in k_{sed}. The observed constant value of v_f [cf. *Wollheim et al.*, 2006] thus suggests a fairly constant sediment denitrification rate constant k_{sed} across systems. While this is an interesting observation, it needs to be evaluated further using reach-scale measurements of k_{sed}, α and v_f.

[43] The variability in α and k_{sed} values represent fluvial systems with varying hydrologic, geomorphic, and biogeochemical attributes. Large α value may be representative of sandy gravelly sediments, while small α values are typical of "muddy" sediments. Sediment and soil organic carbon content (OC) variations exert dominant control on k_{sed} [e.g., *Reddy et al.*, 1982; *Reddy and DeLaune*, 2008]. Thus, large k_{sed} values are representative of sediments with high OC, and low dissolved oxygen that are typical of "impacted" streams draining agricultural lands [*Inwood et al.*, 2005; *Arango et al.*, 2007; *Arango and Tank*, 2008]. Small k_{sed} values, on the other hand, maybe representative of sandy and gravelly sediments with low OC typical of "pristine" streams. Despite such large variability in stream characteristics, the convergence to a robust, inverse stage dependence provides a compelling argument that hydrologic controls dominate over local-scale sediment biogeochemical attributes.

7.2. Scaling of k-h Relationship for the River Network

[44] The motivation of this exploration was to understand how the local k-h relationship, observed in stream tracer experiments under steady flow conditions, scales up in time (k_t-h_{mean} relationship; block C, Figure 1) and space (k_{st}-h_{mean} relationship; block D, Figure 1). There was a surprising consistency in both the spatial and temporal scaling of local k-h dynamics in the stream network.

[45] Analytical modeling indicated that for the same mean annual discharge, there is more processing (higher k_t) in "flashy" streams ($\lambda/k_c < 1$) with high variability in Q than in "damped" streams ($\lambda/k_c > 1$) with low variability in Q. This is because in a more variable or "flashy" system, high-discharge events, characterized by less in-stream processing, are rare and of short duration, and as such they do not contribute much to the overall reduction in nutrient removal. If these high Q values are distributed more uniformly over the year in a "damped" system, the stage is consistently high leading to low removal. Our results also suggest that the intra-annual pdf of Q had no effect on the mean annual removal in "damped" streams, and the temporally averaged k_t-h_{mean} relationship collapses to the underlying k-h relationship. In contrast, in "flashy" streams, the intra-annual pdf of Q significantly affects the mean annual removal. In such systems, the temporally averaged k_t-h_{mean} relationship is different from the underlying k-h relationship, with the difference between the two functions increasing nonlinearly with decrease in λ/k_c. Thus, in "damped" systems the mean annual removal can be estimated based solely on the mean stage and the underlying k-h relationship, making predictions easier. In "flashy" streams additional information is required on the intra-annual pdf of Q which affects the k_t-h_{mean} relationship.

[46] The network models we used to further explore the scaling question were restricted to domains with low intra-annual variability in Q ($\lambda/k_c > 1$). Consistent with the analytical study, the network model indicated that the exponent of the k-h relationship was independent of spatial and temporal averaging scales. Scale dependence was, however, observed in the coefficient, a, of the k-h relationship. We offer preliminary explanations for this observation in section 5, but recognize this as an area of future study. The relatively constant a value with spatial and temporal averaging is intuitively obvious since we are starting with a power function relationship and scaling it up over a fractal river network. If we started with other functional forms between k and h (e.g., exponential), the functional form of the relationship would change with spatiotemporal averaging. The consistency with which the relationship scales up is promising and indicates that it might be possible to estimate in-stream removal without spatially distributed network analysis.

7.3. Prediction of Interannual Variability of k

[47] The analytical model proposed by *Botter et al.* [2010] adequately described the intra-annual pdf of k produced from reanalysis of the MARB simulations generated by *Donner et al.* [2004]. The ability of the stochastic approach to capture the intra-annual pdf of k that is generated using a spatially explicit network model at such large scales (>10,000 km^2) is encouraging, even if the predictions were not exact.

7.4. Implications and Further Work

[48] The biogeochemical scaling of solute removal in streams is interesting and consistent with similar scaling observed for hydrologic attributes.. The results imply that in-stream removal can be described adequately using simple scaling relationships, and without requiring a spatially explicit network model. However, our conclusions are based on comparisons with outputs from network models, and not measured data. This is because of a lack of network-scale data for evaluating nitrogen removal dynamics. Almost all of the data available are at the scale of a single reach, making projections at the network scale entirely model-dependent. To overcome this, in-stream removal data at nested locations within stream networks at different times need to be gathered. The modeling was restricted to streams with low intra-annual variability in Q. We recognize the need for more careful analysis in networks with high Q variability; however, other issues (e.g., temperature effects, ephemeral streams) need to be considered in such analysis.

[49] Our analysis is based on a two-compartment model with a hyporheic transient storage zone while recent studies have shown [*Briggs et al.*, 2010; *Marion et al.*, 2008] that a three-compartment model with an additional transient storage

zone in the water column captures the dynamics of in-stream removal better. However, as noted by *Stewart et al.* [2011], the hyporheic transient storage zone has greater influence on nutrient removal than the surface transient storage zone because of longer residence times. The surface transient storage zone is more critical for plant uptake while our focus was on denitrification. Scaling relationships for N uptake by plants is also of interest; however, such studies would have to consider additional factors like timescales of recycling versus timescale of averaging, as well as how uptake changes along a river network. Finally, though we have focused on nitrate for this manuscript, similar analyses can be developed for any reactive solute based on solute-specific reactivity and the site of occurrence of the reaction (e.g., within channel or in the sediment).

[50] **Acknowledgments.** The contributions of Nandita Basu and Natalia Loukinova were supported by the University of Iowa, while the contributions of Suresh Rao were supported by the Lee A. Reith Endowment and Purdue University. Work on this paper commenced during the Summer Institute organized at the University of British Columbia during June–July 2009 as part of the NSF-funded project: *Water Cycle Dynamics in a Changing Environment: Advancing Hydrologic Science through Synthesis* (NSF grant EAR-0636043, M. Sivapalan, PI). We acknowledge the support and advice of numerous participants at the Summer Institute. Logistic and intellectual support provided by the host for the Summer Institute, Marwan Hassan at University of British Columbia, Canada, is much appreciated.

References

Alexander, R. B., R. A. Smith, and G. E. Schwarz (2000), Effect of stream channel size on the delivery of nitrogen to the Gulf of Mexico, *Nature*, *403*, 758–761, doi:10.1038/35001562.

Alexander, R. B., J. K. Böhlke, E. W. Boyer, M. B. David, J. W. Harvey, P. J. Mulholland, S. P. Seitzinger, C. R. Tobias, C. Tonitto, and W. M. Wollheim (2009), Dynamic modeling of nitrogen losses in river networks unravels the coupled effects of hydrological and biogeochemical processes, *Biogeochemistry*, *93*, 91–116, doi:10.1007/s10533-008-9274-8.

Algoazany, A. S. (2006), Long-term effects of agricultural chemicals and management practices on water quality in a subsurface drained watershed, Ph.D. thesis, Univ. of Ill. at Urbana-Champaign, Urbana.

Arango, C. P., and J. L. Tank (2008), Land use influences the spatiotemporal controls on nitrification and denitrification in headwater streams, *J. N. Am. Benthol. Soc.*, *27*, 90–107, doi:10.1899/07-024.1.

Arango, C. P., J. L. Tank, J. L. Schaller, T. V. Royer, M. J. Bernot, and M. B. David (2007), Benthic organic carbon influences denitrification in streams with high nitrate concentration, *Freshwater Biol.*, *52*, 1210–1222, doi:10.1111/j.1365-2427.2007.01758.x.

Battin, T. J., L. A. Kaplan, S. Findlay, C. S. Hopkinson, E. Mart, A. I. Packman, J. D. Newbold, and F. Sabater (2008), Biophysical controls on organic carbon fluxes in fluvial networks, *Nat. Geosci.*, *1*(2), 95–100, doi:10.1038/ngeo101.

Bencala, K. E., and R. A. Walters (1983), Simulation of solute transport in a mountain pool-and-riffle stream: A transient storage model, *Water Resour. Res.*, *19*(3), 718–724, doi:10.1029/WR019i003p00718.

Böhlke, J. K., R. Antweiler, J. W. Harvey, A. E. Laursen, L. K. Smith, R. L. Smith, and M. A. Voytek (2008), Multi-scale measurements and modeling of denitrification in streams with varying flow and nitrate concentration in the upper Mississippi River basin, USA, *Biogeochemistry*, *93*, 117–141, doi:10.1007/s10533-008-9282-8.

Botter, G., A. Porporato, I. Rodriguez-Iturbe, and A. Rinaldo (2007a), Basin-scale soil moisture dynamics and the probabilistic characterization of carrier hydrologic flows: Slow, leaching-prone components of the hydrologic response, *Water Resour. Res.*, *43*, W02417, doi:10.1029/2006WR005043.

Botter, G., F. Peratoner, A. Porporato, I. Rodriguez-Iturbe, and A. Rinaldo (2007b), Signatures of large-scale soil moisture dynamics on streamflow statistics across U.S. climate regimes, *Water Resour. Res.*, *43*, W11413, doi:10.1029/2007WR006162.

Botter, G., S. Zanardo, A. Porporato, I. Rodriguez-Iturbe, and A. Rinaldo (2008), Ecohydrological model of flow duration curves and annual minima, *Water Resour. Res.*, *44*, W08418, doi:10.1029/2008WR006814.

Botter, G., N. B. Basu, S. Zanardo, P. S. C. Rao, and A. Rinaldo (2010), Stochastic modeling of nutrient losses in streams: Interactions of climatic, hydrologic, and biogeochemical controls, *Water Resour. Res.*, *46*, W08509, doi:10.1029/2009WR008758.

Boyer, E. W., R. B. Alexander, W. J. Parton, C. Li, K. Buterbach-Bahl, S. D. Donner, R. W. Skaggs, and S. J. Del Grosso (2006), Modeling denitrification in terrestrial and aquatic ecosystems at regional scales, *Ecol. Appl.*, *16*, 2123–2142, doi:10.1890/1051-0761(2006)016[2123:MDITAA]2.0.CO;2.

Briggs, M. A., M. N. Gooseff, B. J. Peterson, K. Morkeski, W. M. Wollheim, and C. S. Hopkinson (2010), Surface and hyporheic transient storage dynamics throughout a coastal stream network, *Water Resour. Res.*, *46*, W06516, doi:10.1029/2009WR008222.

Diaz, R. J., and R. Rosenberg (2008), Spreading dead zones and consequences for marine ecosystems, *Science*, *321*, 926–929, doi:10.1126/science.1156401.

Donner, S. D., M. T. Coe, J. D. Lenters, T. E. Twine, and J. A. Foley (2002), Modeling the impact of hydrologic changes on nitrate transport in the Mississippi River Basin from 1955 to 1994, *Global Biogeochem. Cycles*, *16*(3), 1043, doi:10.1029/2001GB001396.

Donner, S. D., C. J. Kucharik, and M. Oppenheimer (2004), The influence of climate on in-stream removal of nitrogen, *Geophys. Res. Lett.*, *31*, L20509, doi:10.1029/2004GL020477.

Doyle, M. W. (2005), Incorporating hydrologic variability into nutrient spiraling, *J. Geophys. Res.*, *110*, G01003, doi:10.1029/2005JG000015.

Doyle, M. W., E. H. Stanley, and J. M. Harbor (2003), Hydrogeomorphic controls on phosphorus retention in streams, *Water Resour. Res.*, *39*(6), 1147, doi:10.1029/2003WR002038.

Durhan, E. J., C. S. Lambright, E. A. Makynen, J. Lazorchak, P. C. Hartig, V. S. Wilson, L. E. Gray, and G. T. Ankley (2006), Identification of metabolites of trenbolone acetate in androgenic runoff from a beef feedlot, *Environ. Health Perspect.*, *114*, 65–68, doi:10.1289/ehp.8055.

Ensign, S. H., and M. W. Doyle (2006), Nutrient spiraling in streams and river networks, *J. Geophys. Res.*, *111*, G04009, doi:10.1029/2005JG000114.

Fuortes, L., M. K. Clark, H. L. Kirchner, and E. M. Smith (1997), Association between female infertility and agricultural work history, *Am. J. Ind. Med.*, *31*, 445–451.

Galloway, J. N., A. R. Townsend, J. W. Erisman, M. Bekunda, Z. Cai, J. R. Freney, L. A. Martinelli, S. P. Seitzinger, and M. A. Sutton (2008), Transformation of the nitrogen cycle: Recent trends, questions, and potential solutions, *Science*, *320*(5878), 889–892.

Green, H. M., K. J. Beven, K. Buckley, and P. C. Young (1994), Pollution incident prediction with uncertainty, in *Mixing and Transport in the Environment*, edited by K. J. Beven, P. C. Chatwin, and J. H. Millbank, pp. 113–137, John Wiley, New York.

Gruber, N., and J. N. Galloway (2008), An Earth system perspective of the global nitrogen cycle, *Nature*, *451*(7176), 293–296.

Hart, D. R. (1995), Parameter estimation and stochastic interpretation of the transient storage model for solute transport in streams, *Water Resour. Res.*, *31*(2), 323–328, doi:10.1029/94WR02739.

Harvey, J. W., B. J. Wagner, and K. E. Bencala (1996), Evaluating the reliability of the stream tracer approach to characterize stream-subsurface water exchange, *Water Resour. Res.*, *32*(8), 2441–2452, doi:10.1029/96WR01268.

Hoellein, T. J., J. L. Tank, E. J. Rosi-Marshall, S. A. Entrekin, and G. A. Lamberti (2007), Controls on spatial and temporal variation of nutrient uptake in three Michigan headwater streams, *Limnol. Oceanogr.*, *52*(5), 1964–1977, doi:10.4319/lo.2007.52.5.1964.

Inwood, S. E., J. L. Tank, and M. J. Bernot (2005), The influence of land use on sediment denitrification in 9 Midwestern streams, *J. N. Am. Benthol. Soc.*, *24*, 227–245, doi:10.1899/04-032.1.

Kemp, W. M., J. M. Testa, D. J. Conley, D. Gilbert, and J. D. Hagy (2009), Temporal responses of coastal hypoxia to nutrient loading and physical controls, *Biogeosciences*, *6*, 2985–3008, doi:10.5194/bg-6-2985-2009.

Leopold, L. B., and T. Maddock Jr. (1953), The hydraulic geometry of stream channels and some physiographic implications, *U.S. Geol. Surv. Prof. Pap.*, *252*.

Marcé, R., and J. Armengol (2009), Modeling nutrient in-stream processes at the watershed scale using nutrient spiralling metrics, *Hydrol. Earth Syst. Sci.*, *13*, 953–967, doi:10.5194/hess-13-953-2009.

Marion, A., M. Zaramella, and A. I. Packman (2003), Parameter estimation of the transient storage model for stream-subsurface exchange,

J. Environ. Eng., *129*(5), 456–463, doi:10.1061/(ASCE)0733-9372(2003)129:5(456).

Marion, A., M. Zaramella, and A. Bottacin-Busolin (2008), Solute transport in rivers with multiple storage zones: The STIR model, *Water Resour. Res.*, *44*, W10406, doi:10.1029/2008WR007037.

McKerchar, A. I., R. P. Ibbitt, S. L. R. Brown, and M. J. Duncan (1998), Data for Ashley River to test channel network and river basin heterogeneity concepts, *Water Resour. Res.*, *34*(1), 139–142, doi:10.1029/97WR02573.

Mitchell, J. K., et al. (2000), Nitrate in river and subsurface drainage flows from an east central Illinois watershed, *Trans. ASAE*, *43*(2), 337–342.

Mulholland, P. J., and D. L. DeAngelis (2000), Surface-subsurface exchange and nutrient spiraling, in *Streams and Ground Waters*, edited by J. B. Jones and P. J. Mulholland, pp. 149–166, Academic, San Diego, Calif., doi:10.1016/B978-012389845-6/50007-7.

Mulholland, P. J., et al. (2008), Stream denitrification across biomes and its response to anthropogenic nitrate loading, *Nature*, *452*, 202–205, doi:10.1038/nature06686.

Osterman, L. E., R. Z. Poore, P. W. Swazenski, D. B. Senn, and S. F. DiMarco (2009), The 20th-century development and expansion of Louisiana shelf hypoxia, Gulf of Mexico, *Geo Mar. Lett.*, *29*, 405–414, doi:10.1007/s00367-009-0158-2.

Rabalais, N. N., R. E. Turner, R. J. Diaz, and D. Justic (2009), Global change and eutrophication of coastal waters, ICES *J. Mar. Sci.*, *66*(7), 1528–1537, doi:10.1093/icesjms/fsp047.

Rabalais, N. N., R. J. Diaz, L. A. Levin, R. E. Turner, D. Gilbert, and J. Zhang (2010), Dynamics and distribution of natural and human-caused hypoxia, *Biogeosciences*, *7*, 585–619, doi:10.5194/bg-7-585-2010.

Reddy, K. R., and R. D. DeLaune (2008), *Biogeochemistry of Wetlands: Science and Applications*, CRC Press, Boca Raton, Fla., doi:10.1201/9780203491454.

Reddy, K. R., P. S. C. Rao, and R. E. Jessup (1982), The effect of carbon mineralization and denitrification kinetics in mineral and organic soils, *Soil Sci. Soc. Am. J.*, *46*, 62–68, doi:10.2136/sssaj1982.03615995004600010011x.

Reggiani, P., M. Sivapalan, and S. M. Hassanizadeh (1998), A unifying framework for catchment thermodynamics: Balance equations for mass, momentum, energy and entropy, and the second law of thermodynamics, *Adv. Water Resour.*, *22*, 367–398, doi:10.1016/S0309-1708(98)00012-8.

Reggiani, P., S. M. Hassanizadeh, M. Sivapalan, and W. G. Gray (1999), A unifying framework for watershed thermodynamics: Constitutive relationships, *Adv. Water Resour.*, *23*, 15–39, doi:10.1016/S0309-1708(99)00005-6.

Reggiani, P., M. Sivapalan, S. M. Hassanizadeh, and W. G. Gray (2001), Coupled equations for mass and momentum balance in a bifurcating stream channel network: Theoretical derivation and computational experiments, *Proc. R. Soc. London, Ser. A*, *457*, 157–189, doi:10.1098/rspa.2000.0661.

Rodriguez-Iturbe, I., and A. Rinaldo (1997), *Fractal River Basins: Chance and Self Organization*, Cambridge Univ. Press, Cambridge, U. K.

Runkel, R. L. (1998), One-Dimensional Transport with Inflow and Storage (OTIS): A solute transport model for streams and rivers, *U.S. Geol. Surv. Water Resour. Invest. Rep.*, *98-4018*. (Available at http://co.water.usgs.gov/otis.)

Runkel, R. L., and S. C. Chapra (1993), An efficient numerical solution of the transient storage equations for solute transport in small streams, *Water Resour. Res.*, *29*(1), 211–215, doi:10.1029/92WR02217.

Schilling, K. E., and R. D. Libra (2000), The relationship of nitrate concentrations in streams to row crop land use in Iowa, *J. Environ. Qual.*, *29*(6), 1846–1851, doi:10.2134/jeq2000.00472425002900060016x.

Smith, V. H. (2003), Eutrophication of freshwater and coastal marine ecosystems a global problem, *Environ. Sci. Pollut. Res.*, *10*(2), 126–139, doi:10.1065/espr2002.12.142.

Soto, A. M., et al. (2004), Androgenic and estrogenic activity in water bodies receiving cattle feedlot effluent in eastern Nebraska, USA, *Environ. Health Perspect.*, *112*, 346–352, doi:10.1289/ehp.6590.

Stewart, R. J., W. M. Wollheim, M. N. Gooseff, M. A. Briggs, J. M. Jacobs, B. J. Peterson, and C. Hopkinson (2011), Separation of river network scale nitrogen removal among main channel and two transient storage compartments, *Water Resour. Res.*, doi:10.1029/2010WR009896, in press.

Stream Solute Workshop (1990), Concepts and methods for assessing solute dynamics in stream ecosystems, *J. N. Am. Benthol. Soc.*, *9*, 95–119, doi:10.2307/1467445.

Tank, J. L., E. J. Rosi-Marshall, M. A. Baker, and R. O. Hall Jr. (2008), Are rivers just big streams? A pulse method to quantify nitrogen demand in a large river, *Ecology*, *89*(10), 2935–2945, doi:10.1890/07-1315.1.

Thomas, S. A., H. M. Valett, J. R. Webster, and P. J. Mulholland (2003), A regression approach to estimating reactive solute uptake in advective and transient storage zones of stream ecosystems, *Adv. Water Resour.*, *26*, 965–976, doi:10.1016/S0309-1708(03)00083-6.

Wagner, B. J., and S. M. Gorelick (1986), A statistical methodology for estimating transport parameters: Theory and applications to one-dimensional advective-dispersive systems, *Water Resour. Res.*, *22*(8), 1303–1315, doi:10.1029/WR022i008p01303.

Winchester, P. D., J. Huskins, and J. Ying (2009), Agrichemicals in surface water and birth defects in the United States, *Acta Paediatr.*, *98*(4), 664–669.

Wollheim, W. M., C. J. Vörösmarty, B. J. Peterson, S. P. Seitzinger, and C. S. Hopkinson (2006), Relationship between river size and nutrient removal, *Geophys. Res. Lett.*, *33*, L06410, doi:10.1029/2006GL025845.

N. B. Basu and N. V. Loukinova, Department of Civil and Environmental Engineering, University of Iowa, Iowa City, IA 52242-1527, USA. (nandita-basu@uiowa.edu)

S. D. Donner, Department of Geography, University of British Columbia, Vancouver, BC V6T 1Z4, Canada.

P. S. C. Rao, School of Civil Engineering, Purdue University, West Lafayette, IN 47907-2051, USA.

M. Sivapalan, Department of Civil and Environmental Engineering, University of Illinois at Urbana-Champaign, Urbana, IL 61801, USA.

S. E. Thompson, Nicholas School of the Environment, Duke University, Durham, NC 27701, USA.

S. Ye, Department of Geography, University of Illinois at Urbana-Champaign, Urbana, IL 61801, USA.